Experimental study of sensitivity-aided application of artificial boundary condition frequencies for damage identification

Experimental study of sensitivity-aided application of artificial boundary condition frequencies for damage identification

Lei Mao[1]*, Yong Lu[2]

[1] Department of Aeronautical and Automotive Engineering, Loughborough University, Epinal Way, Loughborough, LE11 3TU, UK

[2] Institute for Infrastructure and Environment, School of Engineering, The University of Edinburgh, Edinburgh EH9 3JL, UK

*Corresponding author: l.mao@lboro.ac.uk

Abstract

This paper presents an experimental study on the application of the so-called artificial boundary condition (ABC) frequencies for structural damage identification. Aided by the corresponding sensitivity analysis, more suitable ABC frequencies can be selected for improved identification of structural damage. An overview of the theoretical background of ABC frequencies and their sensitivity formulation is provided first. An experimental programme involving model steel beams in the intact and damaged states for the measurements of ABC frequency is presented, and the extraction of the ABC frequencies is descried and discussed. The extracted ABC frequencies are selected in accordance with the sensitivity analysis and they are subsequently employed to identify the structural damage. Results demonstrate that, aided by the sensitivity-based selection procedure, the ABC frequencies can be used for practical identification of structural damage and both the damage location and severity can be determined with good accuracy.

Key words: damage identification, ABC frequency, sensitivity analysis, genetic algorithm

1. Introduction

In recent years, a lot of studies have been devoted to structural health monitoring and damage identification with model-based methods, particularly the finite element (FE) model updating techniques [1-10]. Many FE model updating techniques have been demonstrated to exhibit satisfactory identification performance in the numerical studies. However, in physical structures, measurement and environmental noises often dictate that only a limited amount of modal data, including natural frequencies, mode shapes and damping ratios, may be available with acceptable accuracy [11,15], and this restricts the extent to which damage may be identified from a model updating procedure.

Several studies have been conducted on structural damage identification using experimentally determined natural frequencies [2-4], and it has been found that damages in relatively simple structures, such as 1-dimensional beams, may be identified using the first few natural frequencies. In some latest studies (e.g. [10]), the natural frequencies of higher order modes have been used to identify the local damages in beam-like structures, and the results demonstrate that even small damages could be identified when higher order natural frequencies became available. However, for complex damage identification problems with a large number of variable parameters, using natural frequencies alone would not be sufficient, as the number of natural frequencies is still limited.

Similarly, mode shapes may be measured with good accuracy for relatively simple cases [12-14]; but even for simple structures problems can arise in measuring high modes if the structure is relatively stiff, or when significant nonlinearities are involved. Moreover, pronounced structural damage may cause variation of mode order and this can complicate an accurate determination of higher-order mode shapes. Therefore, it would be desirable if

48 additional modal information can be generated within the lower-order mode region for the
49 general damage detection and structural identification.

50 In the above respect, alternative methods have been proposed to enhance the dataset of modal
51 information for structural damage identification [16-19], including the incorporation of ABC
52 frequencies which are essentially the perturbed natural frequencies of a structure with
53 additional virtual supports. Several studies have been performed using ABC frequencies, as
54 well as antiresonance frequencies, to identify structural damages, and results demonstrate that
55 effective damage identification can be achieved with the use of such frequencies [20-25].

56 Despite the above advancements, the performance of using ABC frequencies from real
57 measurements for damage identification has not been systematically studied. Moreover, since
58 a large variety of perturbed boundary conditions, i.e. the ABC pin supports, may be
59 configured for the ABC frequencies, the inherent information with the ABC frequencies
60 requires further investigation so that more suitable ABC frequencies can be selected to ensure
61 better identification performance. However, only limited research in the literature has been
62 devoted to the selection of ABC frequency for damage identification [23, 26].

63 In this paper, an experimental investigation into the extraction and application of the ABC
64 frequencies for structural damage identification, aided by the sensitivity analysis of the ABC
65 frequencies, is presented. An overview of the background theory about ABC frequency and
66 the theoretical formulation of the ABC frequency sensitivity is provided first. The experiment
67 was performed on model steel beams in the intact and damaged states, and dynamic
68 measurements were taken for the processing and extraction of the ABC frequencies.
69 Extracted ABC frequencies are presented and discussed. Subsequently, the extracted ABC
70 frequencies are selected in accordance with the sensitivity analysis for the incorporation in
71 the FE model updating procedure to identify the structural damage. Results demonstrate that

it is possible to extract ABC frequencies from the experimental, and aided with a sensitivity based selection procedure, the ABC frequencies can be used for the identification of structural damage effectively and both the damage location and severity can be determined with good accuracy.

2. Theoretical background of ABC frequency

Modal frequencies of a given structure with perturbed support conditions provide extra modal information which may be incorporated to enhance the response dataset for structural damage identification. The practicality of such an idea is hindered by the fact that imposing added supports physically on a structure is not normally feasible. Gordis [17, 20] introduced a theoretical approach by which a structure under a supposed set of additional pin supports can be derived from an incomplete frequency response function matrix measured from the original structure, without the need of actually imposing the additional pin supports, and hence the term of artificial boundary condition or ABC frequencies. Expressing the steady state response of a linear system at a forcing frequency ω (rad/s) in the following form:

$$\left(\begin{bmatrix} \mathbf{k}_{mm} & \mathbf{k}_{mo} \\ \mathbf{k}_{om} & \mathbf{k}_{oo} \end{bmatrix} - \omega^2 \begin{bmatrix} \mathbf{m}_{mm} & \mathbf{m}_{mo} \\ \mathbf{m}_{om} & \mathbf{m}_{oo} \end{bmatrix} \right) \begin{Bmatrix} \mathbf{x}_m \\ \mathbf{x}_o \end{Bmatrix} = \begin{Bmatrix} \mathbf{f}_m \\ \mathbf{f}_o \end{Bmatrix} \tag{1}$$

where $\mathbf{k}$ and $\mathbf{m}$ are stiffness and mass matrices, $\mathbf{x}$ and $\mathbf{f}$ are vectors of generalized response and excitation amplitudes, respectively. Subscript 'm' represents measured coordinates or DOFs and subscript 'o' refers to the unmeasured DOFs (‘omitted coordinate set’ or OCS). The OCS is effectively a reduced system, where all the measured DOFs are restrained or pinned to the ground.

Introducing the impedance matrix, $\mathbf{Z} = \mathbf{k} - \omega^2 \mathbf{m}$, Eq. (1) can be re-written as:

$$\begin{bmatrix} \mathbf{Z}_{mm} & \mathbf{Z}_{mo} \\ \mathbf{Z}_{om} & \mathbf{Z}_{oo} \end{bmatrix} \begin{Bmatrix} \mathbf{x}_m \\ \mathbf{x}_o \end{Bmatrix} = \begin{Bmatrix} \mathbf{f}_m \\ \mathbf{f}_o \end{Bmatrix} \tag{2}$$

Assuming there exist no excitation on the omitted coordinates, i.e., f_o=0, Eq. (2) can be rearranged as:

$$\mathbf{f}_m = (\mathbf{Z}_{mm} - \mathbf{Z}_{mo}\mathbf{Z}_{oo}^{-1}\mathbf{Z}_{om})(\mathbf{x}_m) \tag{3}$$

Thus:

$$\mathbf{H}_{mm}^{-1} = (\mathbf{Z}_{mm} - \mathbf{Z}_{mo}\mathbf{Z}_{oo}^{-1}\mathbf{Z}_{om}) \tag{4}$$

where $\boldsymbol{f}_m$ is the generalized excitation at the measured coordinates or DOFs, $\boldsymbol{x}_m$ is the generalized response at these DOFs, and $\mathbf{H}_{mm}$ is the frequency response function (FRF) matrix measured from the structure.

From Eq. (4), it can be seen that at the natural frequencies of the OCS, $\mathbf{Z}_{oo}^{-1}$ is singular, so $\mathbf{H}_{mm}^{-1}$ is also singular. This means that by identifying the singularities from the elements of $\mathbf{H}_{mm}^{-1}$, one can determine the natural frequencies of the OCS, i.e., the frequencies of the structure as if it was physically pinned at the measured DOFs. The relationship can be more conveniently illustrated using an example shown in Fig. 1, where (a) shows the actual simply-supported beam, (b) depicts a perturbed boundary condition with two additional pin supports at “i” and “j”, for which the modal frequencies are to be evaluated, and (c) shows the actual measurement settings. Instead of physically imposing the two additional pins as indicated in Fig. 1(b), the modal frequencies under such a boundary condition can be determined by measuring the (2x2) FRF matrix on the original beam at points “i” and “j” shown in Fig. 1(c), and subsequently identifying the singularities from the inverted FRF matrix.

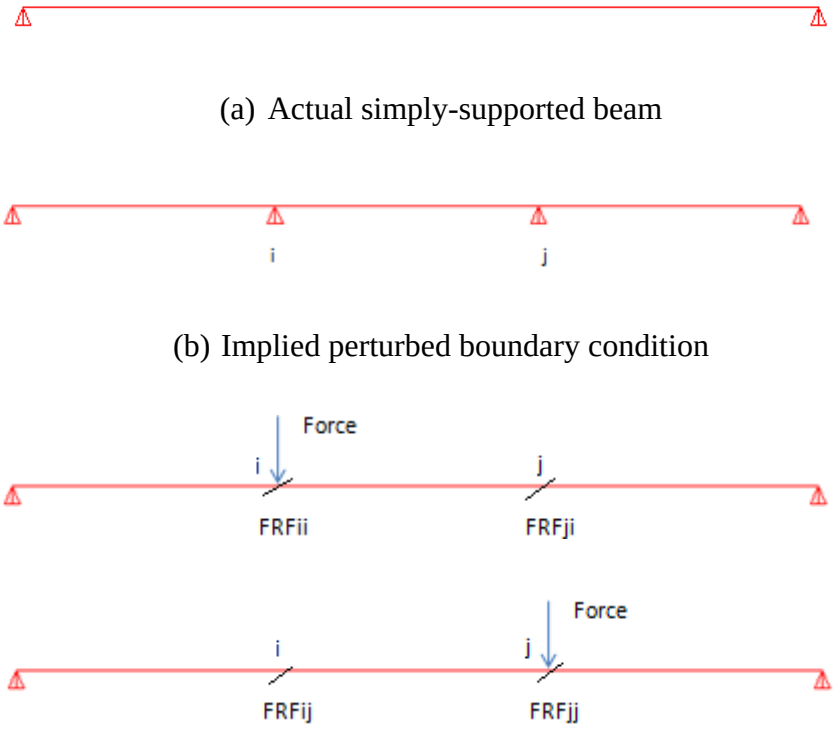

(a) Actual simply-supported beam

(b) Implied perturbed boundary condition

(c) Actual measurements for extraction of ABC frequencies

Figure 1 Illustration of artificial boundary condition frequency measurement settings

3. Overview of the sensitivity formulation and verification

In this section, an overview of the theoretical formulation for the sensitivity of ABC frequencies is provided. In particular, the sensitivity of two-pin ABC frequencies and the underlying mode shape contribution [26] are discussed in connection with the selection of ABC frequencies for damage identification.

3.1 Sensitivity analysis of one-pin ABC frequencies

Based on the concept of the ABC frequencies as briefly described in Section 2, the classical driving-point anti-resonance is effectively the one-pin ABC frequencies. Hence the sensitivity analysis of one-pin ABC frequencies follows the same formulation as the driving-point anti-resonance. From the general definition of the frequency response function (FRF), the driving-point FRF can be expressed as [18]:

133 $$h_{ii}(\omega)=\sum_{k=1}^{n}\frac{\varphi_{ik}\det\left(\Lambda-\omega^2 I\right)_k\varphi_{ik}}{\det\left(\Lambda-\omega^2 I\right)} \quad (5)$$

134 where $\det\left(\Lambda-\omega^2 I\right)_k=\left(\omega_1^2-\omega^2\right)\left(\omega_2^2-\omega^2\right)\cdots\left(\omega_{k-1}^2-\omega^2\right)\left(\omega_{k+1}^2-\omega^2\right)\cdots\left(\omega_n^2-\omega^2\right)$

135 The driving point anti-resonance frequencies, i.e. the one-pin ABC frequencies, denoted by
136 ω_{1-pin_i}, can be obtained by setting Eq.(5) to zero. According to Mottershead [18], the
137 sensitivities of anti-resonance (one-pin ABC) frequencies to a particular structural parameter
138 can be expressed as:

139 $$\frac{\partial\omega_{1-pin\_i}^2}{\partial p}=2\times\frac{\sum_{k=1}^{n}\frac{\partial\varphi_{ik}}{\partial p}\det\left(\Lambda-\omega_{1-pin\_i}^2 I\right)_k\varphi_{ik}}{\sum_{k=1}^{n}\varphi_{ik}\left(\sum_{\substack{p=1\\p\neq k}}^{n}\det\left(\Lambda-\omega_{1-pin\_i}^2 I\right)_{k,p}\right)\varphi_{ik}}+\frac{\sum_{p=1}^{n}\frac{\partial\omega_p^2}{\partial p}\left(\sum_{\substack{k=1\\k\neq p}}^{n}\det\left(\Lambda-\omega_{1-pin\_i}^2 I\right)_{k,p}\varphi_{ik}\varphi_{ik}\right)}{\sum_{k=1}^{n}\varphi_{ik}\left(\sum_{\substack{p=1\\p\neq k}}^{n}\det\left(\Lambda-\omega_{1-pin\_i}^2 I\right)_{k,p}\right)\varphi_{ik}} \quad (6)$$

140 where *p* is the structural parameter, in this study *p* represents the beam element stiffness.

141 Eq. (6) indicates that the sensitivity of the one-pin ABC frequencies is a combination of the
142 sensitivity of mode shape displacement at the same point and the sensitivity of the natural
143 frequencies, all to the same parameter *p*. It is understandable that the localisation capacity of
144 the one-pin ABC frequencies is dependent upon the relative significance of the mode shape
145 contribution in the sensitivity, therefore a relative mode shape contribution ratio as proposed
146 in [19] is adopted here:

147 $$C=\frac{|\Phi|}{|\Omega|+|\Phi|} \quad (7)$$

148 where C is the relative mode shape contribution ratio, Ω denotes the natural frequency
149 contribution and Φ is the mode shape contribution in the one-pin ABC sensitivity. Φ and Ω
150 can be calculated from the first and second term of Eq. 6, respectively.

The (one-pin) ABC frequencies that contain a larger mode shape contribution are expected to be relatively more sensitive to damage and hence should be selected for the FE model updating.

3.2 Sensitivity analysis of two-pin ABC frequencies

The similar line of formulation can be extended to the sensitivity of two-pin ABC frequencies and the determination of the mode shape contributions in the two-pin ABC frequency sensitivities, as discussed in detail in [26]. Let the measured 2×2 FRF matrix be expressed as:

$$H = \begin{bmatrix} h_{ii} & h_{ij} \\ h_{ji} & h_{jj} \end{bmatrix} \tag{8}$$

Inverting the above matrix yields:

$$H^{-1} = \frac{1}{\left| h_{ii}h_{jj} - h_{ij}h_{ji} \right|} \begin{bmatrix} h_{jj} & -h_{ij} \\ -h_{ji} & h_{ii} \end{bmatrix} \tag{9}$$

The singular (peak) frequencies in the inverted matrix, i.e. the two-pin ABC frequencies, can be calculated by setting $\left| h_{ii}h_{jj} - h_{ij}h_{ji} \right|$ to zero. For simplicity and without losing generality, let us consider just the first three modes of the ABC frequencies. The two-pin ABC frequencies with pins at i and j can be represented as:

$$\omega_{2-pin}^2 = \frac{A1\times\omega_3^2 + A2\times\omega_2^2 + A3\times\omega_1^2}{A1 + A2 + A3} \tag{10}$$

where $A1 = \left(\varphi_{i1}\varphi_{j2} - \varphi_{i2}\varphi_{j1}\right)^2$, $A2 = \left(\varphi_{i1}\varphi_{j3} - \varphi_{i3}\varphi_{j1}\right)^2$, $A3 = \left(\varphi_{i2}\varphi_{j3} - \varphi_{i3}\varphi_{j2}\right)^2$

The derivative of the two-pin ABC frequencies with respect to a variable parameter p can be further expressed as follows:

$$\frac{\partial \omega_{2-pin}^2}{\partial p} = \frac{\left(\frac{\partial A1}{\partial p}\omega_3^2 + \frac{\partial \omega_3^2}{\partial p}A1 + \frac{\partial A2}{\partial p}\omega_2^2 + \frac{\partial \omega_2^2}{\partial p}A2 + \frac{\partial A3}{\partial p}\omega_1^2 + \frac{\partial \omega_1^2}{\partial p}A3\right)(A1+A2+A3)}{(A1+A2+A3)^2} - \frac{\left(\frac{\partial A1}{\partial p}+\frac{\partial A2}{\partial p}+\frac{\partial A3}{\partial p}\right)\left(A1\times\omega_3^2 + A2\times\omega_2^2 + A3\times\omega_1^2\right)}{(A1+A2+A3)^2} \quad (11)$$

Accordingly, the natural frequency and mode shape contributions in the two-pin ABC frequency sensitivities can be expressed as:

$$\Phi = \frac{\left(\frac{\partial A1}{\partial p}\omega_3^2 + \frac{\partial A2}{\partial p}\omega_2^2 + + \frac{\partial A3}{\partial p}\omega_1^2 + \right)(A1+A2+A3)}{(A1+A2+A3)^2} - \frac{\left(\frac{\partial A1}{\partial p}+\frac{\partial A2}{\partial p}+\frac{\partial A3}{\partial p}\right)\left(A1\times\omega_3^2 + A2\times\omega_2^2 + A3\times\omega_1^2\right)}{(A1+A2+A3)^2} \quad (12a)$$

$$\Omega = \frac{\left(\frac{\partial \omega_3^2}{\partial p}A1 + \frac{\partial \omega_2^2}{\partial p}A2 + \frac{\partial \omega_1^2}{\partial p}A3\right)(A1+A2+A3)}{(A1+A2+A3)^2} \quad (12b)$$

The relative contribution of the mode shape in the two-pin ABC frequency sensitivities can then be evaluated using Eq. (7). On this basis, the two-pin ABC frequencies can be selected based on their mode shape contributions in structural damage identification.

3.3 Verification of ABC frequency sensitivity

The basic verification of the ABC frequency sensitivity analysis has been presented in [26]. Herein some further verification including multiple locations of damage is briefly descried and discussed.

The beam employed in the simulation for the ABC frequency sensitivity analysis is the same as the experimental steel beam which will be described in Section 4.1. The beam is 1m long, and the cross section is 50 × 6 mm. The beam is fully fixed at both ends. In the analysis, the beam is divided into ten elements, thus nine artificial pin locations are possible. As

representation, two-pin ABC frequencies are considered and for convenience only the first order ABC frequencies are employed in the verification.

In the numerical sensitivity analysis, single and multiple damages are created with 1% stiffness reduction to the different beam elements, and the two-pin ABC frequency sensitivities calculated using the proposed equations in Section 3.2 are compared with those obtained directly from the numerical model with the addition of actual pins.

Figure 2 shows the comparison of the two-pin ABC frequency sensitivities for cases where a single damage location is involved, where the numbers in the x-axis labels indicate the pin positions, for example, “12” means pins located at points 1 and 2. The vertical axis is the sensitivity of the squared two-pin ABC frequency according to Eq. (11). It should be noted that as the beam is divided into 10 elements herein, nine locations can be used for the pin placement (two end points are fixed), thus there exists a large amount of combinations for the two pin positions. Herein only ABC frequency sensitivities with two pins at adjacent points are illustrated . Figure 3 shows the comparison of the two-pin ABC frequency sensitivities for cases where two damages are involved. Owing to the fact that there could be numerous multiple damage combinations, only two damage scenarios are considered herein, namely a) two closely-spaced damages at element between nodes 2 and 3 and element between nodes 4 and 5, and b) two distantly spaced damages at element between nodes 3 and 4 and element between nodes 8 and 9.

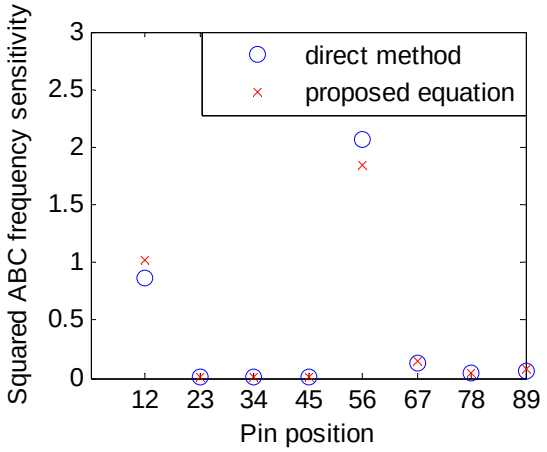

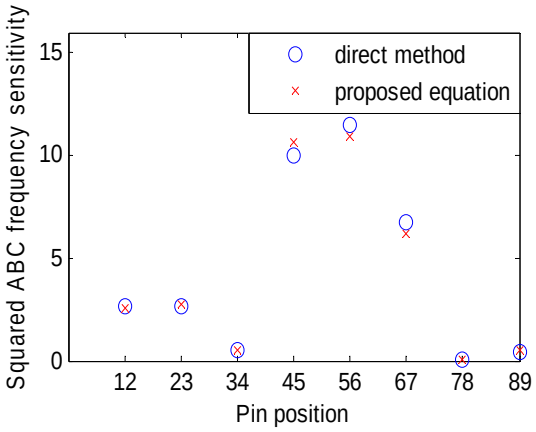

205

206 (a) Damage between nodes 2 and 3 (b) Damage between nodes 6 and 7

207 Figure 2 Verification of two-pin ABC frequency sensitivity calculations for single damage
208 location

209

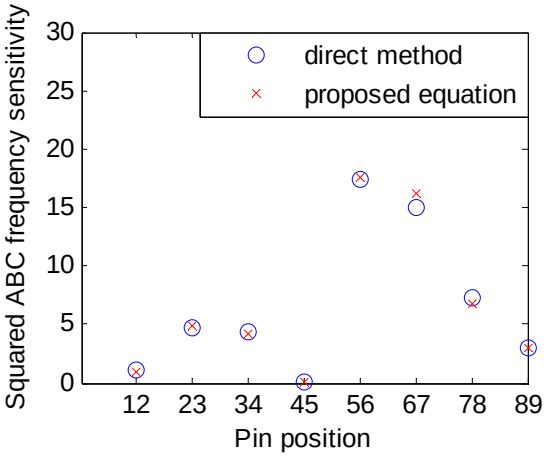

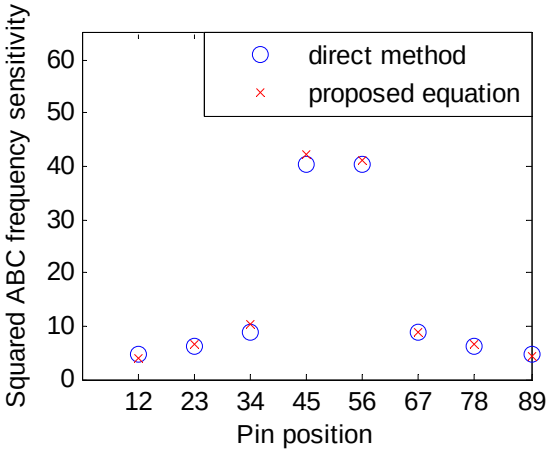

210

211 (a) Closely-spaced damages (b) Distantly-spaced damages

212 Figure 3 Verification of two-pin ABC frequency sensitivity calculations for multiple damage
213 locations

214

215 From Figures 2 and 3, it can be observed that in all cases the two-pin ABC frequency
216 sensitivities calculated using Eq. (11) compare well with the direct results. It should be noted
217 that only the first few modes are employed to calculate the two-pin ABC frequency
218 sensitivity using the equations, and this may be the source of the slight differences in the

comparisons. In general, it can be observed that two-pin ABC frequency sensitivity exhibits marked variation for different pin (ABC) configurations or locations, and this indicates that there is a significant scope for the selection of better suited ABC frequencies for a more reliable damage identification.

4. Experimental programme

A laboratory experimental study has been conducted to investigate the extraction of the ABC frequencies from physical tests and examine the optimal selection of the ABC frequencies for damage identification in the test structures.

4.1 Test structure and test procedure

In this study, a scaled steel beam with a flat cross section was chosen for the experiment. The dimensions of the test beam have been selected so that the modal properties of the test beam were representative of typical beams in civil engineering construction.

Fig. 4 shows the basic test setup and dimensions of the test beams. The steel beams were uniformly 1m long, and the cross section was 50mm wide and 6 mm thick. The test beams were clamped at both ends, simulating fixed-end supports. During the test, each beam was divided into 10 equal segments, so there were 9 measurement points with the exclusion of the two end supports.

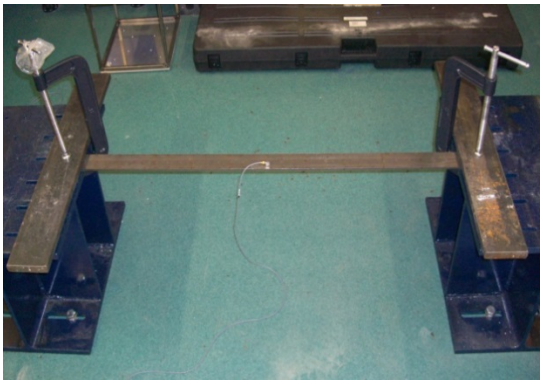

(a) Test beam set-up and attachment of accelerometers

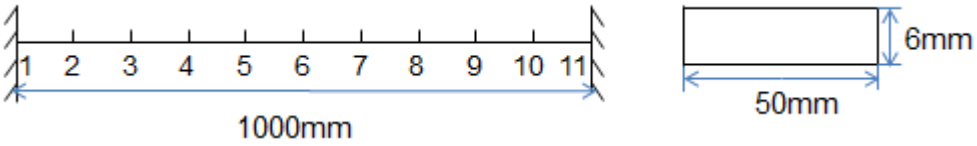

(b) Arrangement of the measurement points for the beam

Figure 4 Test setup for the steel beam

The experiment was carried out following a standard modal testing procedure. An impact hammer was used to excite the test beams. The impact force time history was measured by a built-in load cell in the impact hammer. Meanwhile, the dynamic responses of the test beam were recorded by accelerometers attached to the designated points of the test structure. A sampling frequency of 20 kHz was employed so as to provide enough resolution for the recording of the details of the impact force to ensure a reliable FRF calculation.

The procedure described in Section 2 is used to obtain FRF curves and extract one-pin and two-pin ABC frequencies. It should be noted that several signal processing techniques have been applied to in the process to obtain the FRF curves to reduce the noise influence, including windowing, filtering, averaging, and the singular value decomposition (SVD) procedure. More details of these techniques can be found in [25].

4.2 Extraction of ABC frequencies from the measurements

With the processed FRF curves from the experiment, one-pin and two-pin ABC frequencies can be identified from the elements of the inverted FRF matrix. In this section, the extracted one-pin and two-pin ABC frequencies are examined with the application of the aforementioned data processing techniques.

To generally cover all possible one-pin and two-pin ABC scenarios, a detailed test routine was organized such that a large variety of artificial pin configurations can be obtained by combining the impact and measurement scenarios tested during the experiment.

4.2.1 Experimental one-pin ABC frequencies

For the one-pin cases, the measured FRF matrix reduces to a single driving-point FRF, and the ABC frequencies are actually the anti-resonances in the FRF curves. In line with the general ABC approach, these can be identified from peaks on the inverted driving-point FRF.

Figure 5 depicts three one-pin ABC curves (inverted driving-point FRF) from the test beam, with pin locations distributed along the beam. The extracted one-pin ABC frequencies are compared with those from the numerical predictions by adding one actual pin to the corresponding position in the FE model, the results are listed in Table 1.

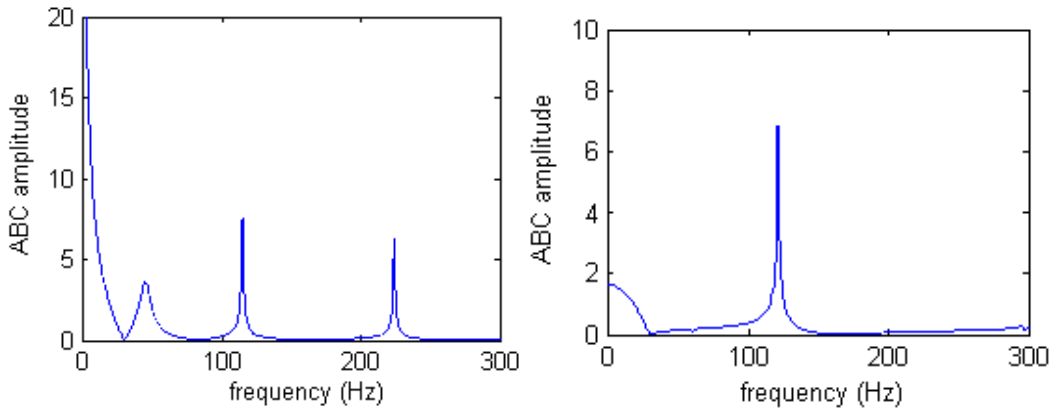

(a) One-pin ABC curve with pin at 3 (b) One-pin ABC curve with pin at 6

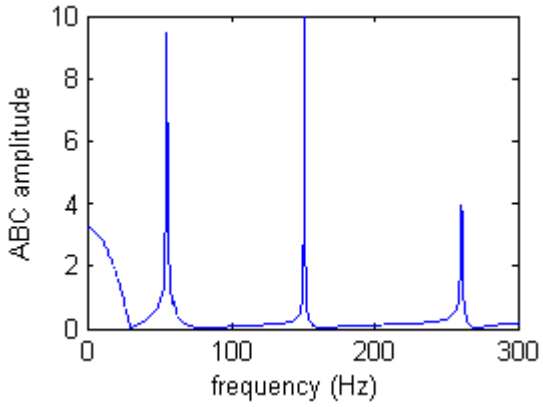

(c) One-pin ABC curve with pin at 8

Figure 5 One-pin ABC curves from the intact test beam

Table 1 One-pin ABC frequencies from the experiment / FE prediction

Pin location	Frequencies (Hz)		
	1st	2nd	3rd
3	39.9 / 38.8	105.2 / 104.8	210.3 / 206.4
6	/ 83.5	122 / 121.1	/270.4
8	54.2 / 53.7	152 / 150	261 / 262.7

From the above results, it can be seen that if the pin is located at the nodal point of a natural mode, the corresponding modal information will not be measured. The implication for the ABC frequencies extraction is that, if that natural mode happens to be an ABC mode as well, such an ABC mode will not be identifiable from that measurement. In this case, as the centre point (location 6 in Figure 2b) is nodal point of the second natural mode, and the mode is also the first ABC mode, only the second ABC frequency can be measured from the test.

For the other measurement cases, the first few one-pin ABC frequencies can be clearly and exclusively identified, and by comparing to those from the prediction by the FE model, it can be said that the one-pin ABC frequencies can be extracted with good accuracy.

4.2.2 Experimental two-pin ABC frequencies

As mentioned earlier, for two-pin ABC frequencies the FRF matrix will be a 2×2 matrix, consisting of four FRF curves. This matrix is then inverted to yield the required $\mathbf{H}_{mm}^{-1}$ matrix, with four elements representing four ABC curves. The ABC frequencies may be identified from any of these curves, and in practice the curves from other elements may be used for cross-checking and assurance purposes.

There are obviously a variety of configurations with arbitrary locations of the two pins. To allow for a systematic observation in a better organised manner, representative pin positions

293 are chosen to cover essentially all possible combinations, with two pins located with various
294 distances.

295 Figure 6 depicts four typical two-pin ABC curves from various measurement configurations
296 ("pin" locations). Similarly, these extracted two-pin ABC frequencies are compared with
297 those from the FE model by adding two actual pins to the same locations, and the results are
298 listed in Table 2.

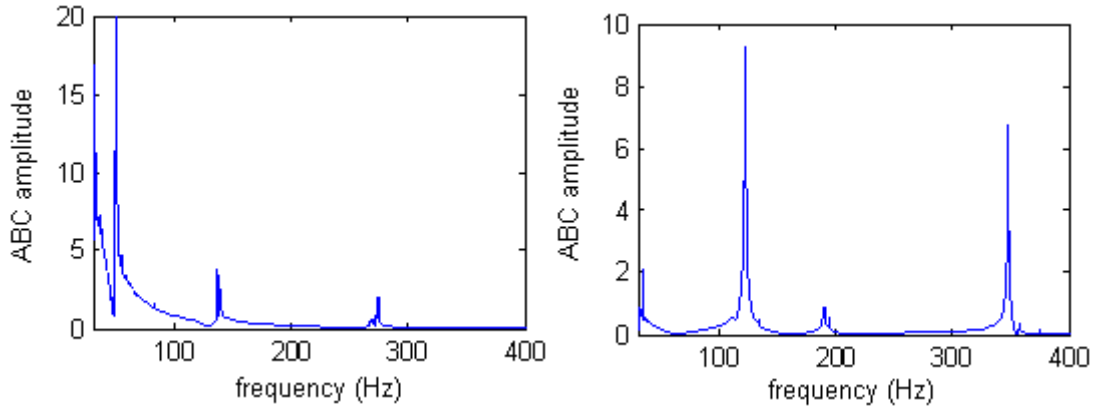

299

300 (a) Pins at node 2 and 3 (b) Pins at node 5 and 7

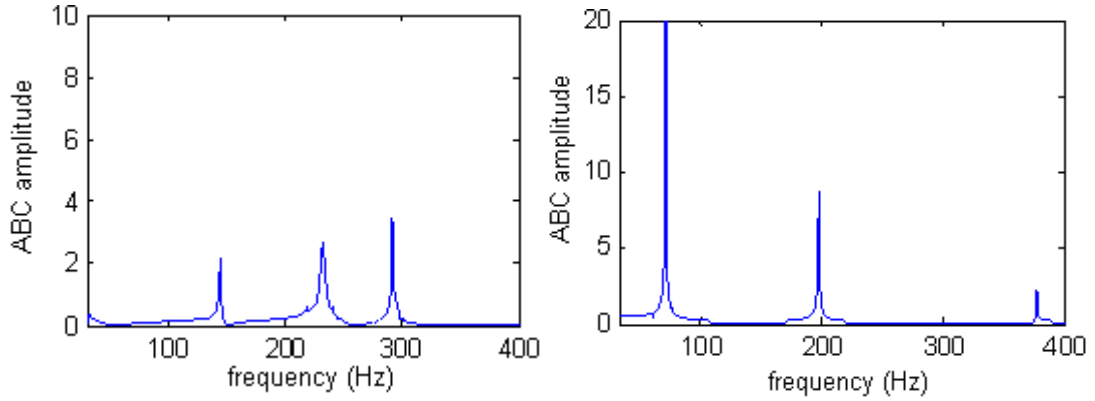

301

302 (c) Pins at 4 and 8 (d) Pins at 3 and 9

303 Figure 6 Two-pin ABC curves from the test beam

304

305

Table 2 Two-pin ABC frequencies from experiment / FE prediction

Pin locations	Frequencies (Hz)		
	1st	2nd	3rd
2,3	50.1 / 48.3	135.5 / 134	271.6 / 263.8
5,7	121.6 / 120.8	190.4 / 191.5	346.8 / 340.7
4,8	141.7 / 139.85	232.8 / 233.3	292.7 / 291.9
3,9	67.3 / 66.8	191.1 / 189.9	374.9 / 373.0

From Fig. 6, the first few peaks can be identified clearly, although the smoothness of these curves is not as good as in the one-pin scenarios, which is quite expected due to the involvement of four FRF functions and the inverting operation. In fact, even in a physical test where two additional pin supports are actually imposed, the frequency response function could be subject to increased “noises” due to the increased rigidity of the beam and the shift of the modal frequencies towards a higher range.

The results described above demonstrate that extracting ABC frequencies for a beam-like structure from a normal modal test is feasible and practical for one-pin and two-pin configurations. These ABC frequencies can then be considered for structural damage identification.

5. Experimental investigation of selecting ABC frequencies in structural damage identification

In this section, the one-pin and two-pin ABC frequencies will be selected based on the the a sensitivity analysis, and selected ABC frequencies will be used to identify damage in the test beam. From the results in Section 3, one-pin and two-pin ABC frequencies containing higher mode shape contribution will be selected for the subsequent application in the damage identification via a finite element model updating procedure.

5.1 Experimental benchmark damaged beam

In this experiment, a damaged beam was created and the ABC frequencies after creating the damage are extracted using the same procedure as described in Section 4 for the undamaged beam.

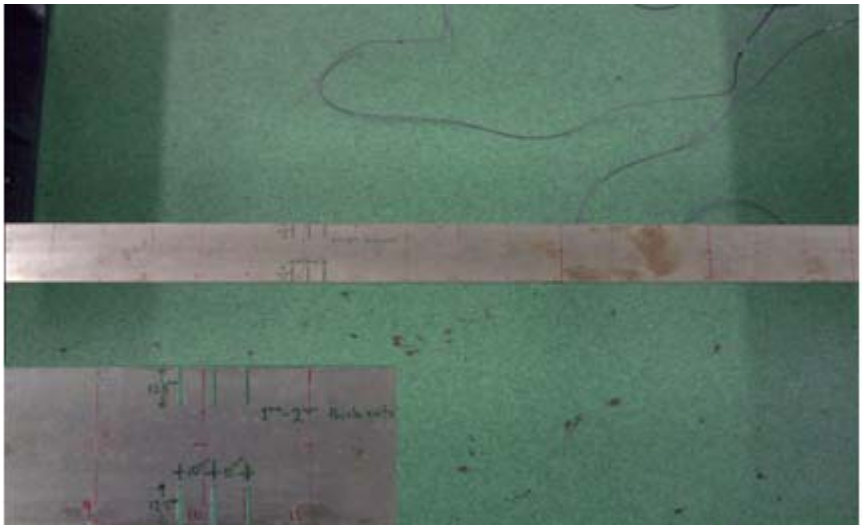

(a) Stiffness reduction (damage) in the test beam

(b) Schematic showing the dimensions of cuts in the beam

Figure 7 Test beam with damage

Figure 7 depicts the damaged test beam. The damage was intended to represent a generic reduction of the stiffness over a fixed area between about 0.33m-0.36m to the left end of the beam. Several cuts were made to create a relatively uniform reduction of the section stiffness over the damaged area, instead of a single cut which would cause a varying stiffness zone in the vicinity of the cut and hence introducing unnecessary complexity for the present evaluation. By creating a (relatively) uniform stiffness reduction area, it also makes an

340 analysis using a simple FE model for comparison more straightforward. With verification
341 from an FE model, the cuts resulted in a reduction of stiffness by about 30% over a length of
342 100mm (10% of the total beam length).

343 The natural frequencies of the damaged beam were measured firstly, and the changes of
344 natural frequencies due to the damage are listed in Table 3. It can be seen that the damage
345 leads to a change (reduction) of the natural frequencies in a range of 0.7-2.7%, with the
346 highest reduction occurring to the second mode. This is expected because the damage
347 location was at about one-third length of the beam.

348 Table 3 Experimental natural frequencies and corresponding changes from the damaged
349 beam

Mode number	1^{st}	2^{nd}	3^{rd}
Experimental (with cuts)	29.8Hz	80.6Hz	161.6Hz
Experimental (without cuts)	30.5Hz	82.9Hz	162.7Hz
Changes due to damages	-2.3%	-2.8%	-0.68%

350

351 5.2 Selection scheme

352 As mentioned earlier, there exists a large amount of ABC pin configurations, especially in
353 two-pin scenarios, it is necessary to make a selection from all available one-pin and two-pin
354 ABC frequencies to achieve better identification results. In this section, the selection scheme
355 proposed in [26] is used for the ABC frequency selection, which can be briefly described
356 below.

357 For a structure with n elements, a total of n sensitivity values for a particular ABC frequency
358 can be obtained, forming a sensitivity vector, S. Defining the sensitivity of the ABC

359 frequency to a damage in the i-th element as Si, the sensitivity vector S can be written as [S]
360 = [S1, S2, …, Sn-1, Sn]. With Eq. (12), the mode shape contribution index C of each ABC
361 frequency sensitivity can be calculated, giving a vector of index [C] = [C1, C2, …, Cn-1, Cn].
362 Based on the mode shape contribution vector C, the overall sensitivity of an ABC frequency
363 may be expressed as:

364 $$\overline{C} = \mu_C + \mu_C / \sigma_C \tag{13}$$

365 where μ_C and σ_C are mean value and standard deviation of the vector C.

366 From index $\overline{C}$, the ABC frequencies with higher mean value and smaller standard deviation
367 value will be selected for the following damage identification, as these ABC frequency
368 sensitivities have collectively higher mode shape contributions to all possible damage
369 scenarios.

370 5.3 Damage identification on the test beam with selected ABC frequencies

371 From Section 5.1, the damage created in the test beam can be expressed with the 30%
372 stiffness reduction at the 4th beam element shown in Figure 2(b). In this Section, a damage
373 identification procedure is performed using the measured ABC frequencies, and the
374 identification results in terms of the location and damage severity will be checked against the
375 about actual damage.

376 The identification is carried out through a FE model updating procedure, and the genetic
377 algorithm (GA) is used to update the beam stiffness with selected ABC frequencies in the
378 process to best match the measured dataset. The parameters used in GA are listed in Table 4,
379 and more details can be found in [23].

380

Table 4 GA configuration

Max generation	1,000
Selection method	Ranking selection
Crossover method	Heuristic crossover
Crossover probability	0.7
Mutation method	Uniform mutation
Mutation probability	0.02

From previous studies, the number of modal data should be 2-3 times the number of parameters being updated in order to achieve a satisfactory result [27]. Therefore, in order to update all of the 10 beam element stiffness values, the minimum 20 one-pin and two-pin ABC frequencies are selected using the methodology described in section 5.2. Figure 8 shows the updated results of the element stiffness and corresponding percentage errors with respect to the actual stiffness distribution in the test beam.

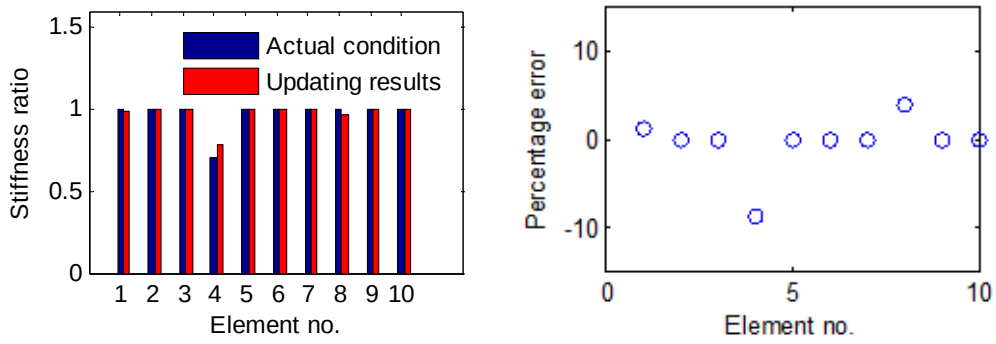

Figure 8 Model updating results using 20 selected ABC frequencies (left) and corresponding percentage errors (right)

It can be seen from Figure 8 that the stiffness ratios for most of the 10 beam elements are predicted within a margin of error of 3%, while the predicted stiffness in the damaged element has an error of less than 10%. The average percentage error in all stiffness parameters is 1.4%. Such results demonstrate that, using experimental ABC frequencies, both

the damage location and the severity could be successfully identified in physical structures when a similar test condition could be achieved.

5.4 Performance of selected ABC frequencies in multiple damage scenarios

From above results, the selected one-pin and two-pin ABC frequencies can identify the single damage in the test beam with good quality. In this section, the performance of selected ABC frequencies in identifying multiple damages is demonstrated.

Similar to the procedure described in Section 5.3, 20 one-pin and two-pin ABC frequencies are selected to update the 10 beam element stiffness using GA. The results are depicted in Figure 9, and the maximum and mean updating errors are listed in Table 5.

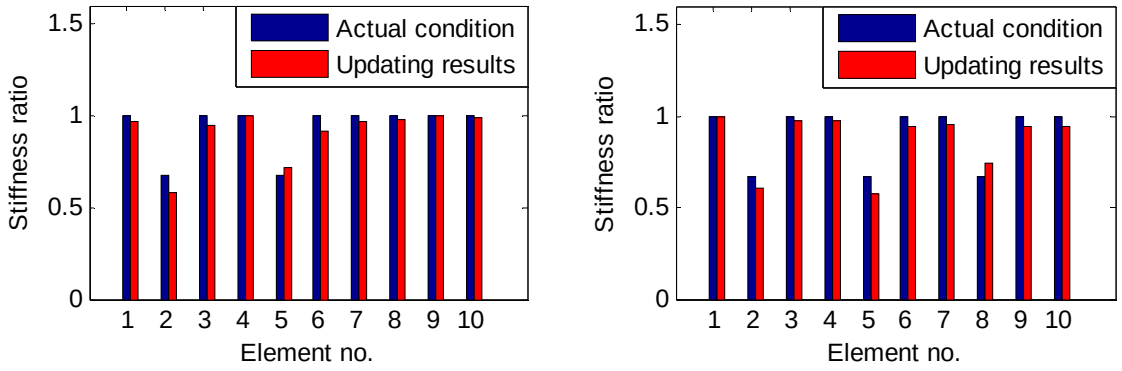

(a) Scenario 1 (b) Scenario 2

Figure 9 Model updating results for multiple damage scenarios

Table 5 Maximum and mean updating errors for multiple damage scenarios

Multiple damage scenario	Maximum updating error	Mean updating error
1	8%	4%
2	9%	4.9%

It can be seen from Figure 8 that with selected ABC frequencies, multiple damages in the test beam can still be identified with good quality, the maximum updating error for multiple damage scenario is still less than 10%, indicating that minor change in the beam performance can be detected using the selected one-pin and two-pin ABC frequencies, this further confirm the robustness of selected ABC frequencies in identifying structural damages.

6. Conclusions

In this paper, an experimental study is presented to investigate the identification of structural damages using selected ABC frequencies based on a sensitivity evaluation with measurements from a physical test structure. The measurement procedure to extract the ABC frequencies and the measurement quality is also discussed.

In accordance with the formulation of the one-pin and two-pin ABC frequency sensitivities, the selection scheme is derived on the basis of the relative contributions of the mode shape coordinates at the pin locations in the ABC frequency sensitivities.

The verification of the sensitivities calculated using the formulations in comparison with those generated from the finite element simulations demonstrate that the calculated ABC frequency sensitivities are sufficiently accurate for both single- and multiple-damage scenarios.

Comparison of the experimentally extracted one-pin and two-pin ABC frequencies from the test beam with those produced from the numerical simulation show that with the described testing procedure and use of the associated data analysis techniques, the first few one-pin and two-pin ABC frequencies from each mode can be extracted with good accuracy.

The ABC frequencies from the measured pool are ranked on the basis of the sensitivity calculations, and those containing high mode shape contributions are selected to the identification of various damages in the test beam through a FE updating procedure. The

identification results show that with the selected one-pin and two-pin ABC frequencies reliable identification results about the damage location and severity for single as well as multiple damage scenarios.

References

[1] Stubbs, N., Broome, T.H., Osegueda, R. Monitoring and Evaluating Civil Structures using Measured Vibration. Proc. 14th International Modal Analysis Conference 1990; 84-90.

[2] Kim, J.T., Stubbs, N. Crack detection in beam-type structures using frequency data. Journal of Sound and Vibration 2003: 259: 145-160.

[3] Hearn, G., Testa, R.B. Modal Analysis for Damage Detection in Structures. Journal of Structural Engineering 1991; 117: 3042-3063.

[4] Messina, A., Williams, E.J., Contursi, T. Structural damage detection by a sensitivity and statistical based method. Journal of Sound and Vibration 1998: 216: 791-808.

[5] Carrasco, C, et al. Localization and Quantification of Damage in a Space Truss Model using Modal Strain Energy. Smart Systems for Bridges, Structures and Highways, Proceedings of SPIE 1997; 3043: 181-192.

[6] Leutenegger, T. Structural Testing of Fatigued Structures. Smart Structures and Integrated Systems. 1999; 3668: 987-997.

[7] Mroz, Z., Lekszynski, T. Identification of Damage in Structures using Parameter Dependent Modal Response. Proceedings of ISMA25, Noise and Vibration Engineering, Leuven, Belgium, 2000.

[8] Koh, B.H., Dyke, S.J. Structural health monitoring for flexible bridge structures using correlation and sensitivity of modal data. Computers and Structures 2007; 85: 117-130.

[9] Gandomi, A.H., Sahab, M.G., Rahaei, A., Safari Gorji, M. Development in Mode Shape-Based Structural Fault Identification Technique. World Applied Science Journal 2008; 5: 29-38.

[10] Stache, M., Guettler, M., Marburg, S. A precise non-destructive damage identification technique of long and slender structures based on modal data. Journal of Sound and Vibration, 2016; 365: 89-101.

[11] Mottershead, J.E., Friswell, M.I. Model Updating in Structural Dynamics: A Survey. Journal of Sound and Vibration 1993;167: 347-375.

[12] Yan, Y.J., Cheng, L., Wu, Z.Y., Yam, L.H. Development in Vibration-based Structural Damage Detection Technique. Mechanical Systems and Signal Processing 2007; 21:2198-2211.

[13] Gandomi, A.H., Sahab, M.G., Rahaei, A., Safari Gorji, M. Development in Mode Shape-Based Structural Fault Identification Technique. World Applied Science Journal 2008;5: 29-38.

[14] Doebling, S.W., Farrar, C.R., Prime, M.B., Shevitz, D.W. Damage Identification and Health Monitoring of Structural and Mechanical Systems from Changes in Their Vibration Characteristics: A Literature Review. Los Alamos National Laboratory, 1996.

[15] Sohn, H., Farrar, C.R., Hemez, F.M., Shunk, D.D., Stinemates, D.W., Nadler, B.R., Czarnecki, J.J. A Review of Structural Health Monitoring Literature: 1996-2001. Los Alamos National Laboratory, 2004.

[16] Li, S., Shelley, S.J., Brown, D.L. Perturbed Boundary Condition Testing Concepts. 13th International Modal Analysis Conference (IMAC), Nashville, Tennessee, 1995;13-16.

[17] Gordis, J.H. Omitted Coordinate Systems and Artificial Constraints in Spatially Incomplete Identification. Modal Analysis 1996;11: 83-95.

[18] Mottershead, J.E. On the Zeros of Structural Frequency Response Functions and Their Sensitivities. Mechanical Systems and Signal Processing, 1998;12: 591-597.

[19] Hanson, D., Waters, T.P., Thompson, D.J., Randall, R.B., Ford, R.A.J. The Role of Anti-resonance Frequencies from Operational Modal Analysis in Finite Element Model Updating. Mechanical Systems and Signal Processing 2007;21: 74-97.

[20] Gordis, J.H. Artificial Boundary Conditions for Model Updating and Damage Detection. Mechanical Systems and Signal Processing 1999;13: 437-448.

[21] Ambrogio, W.D., Fregolent, A. The Use of Antiresonances for Robust Model Updating. Journal of Sound and Vibration 2000; 236: 227-243.

[22] Jones K., Turcotte. J. Finite Element Model Updating using Antiresonant Frequencies. Journal of Sound and Vibration 2002;252: 717-727.

[23] Tu, Z.G., Lu, Y. FE Model Updating using Artificial Boundary Conditions with Genetic algorithms. Computers and Structures 2008; 86: 714-727.

[24] Gordis, J.H., Papagiannakis, K. Optimal selection of artificial Boundary Conditions for model updating and damage detection. Mechanical Systems and Signal Processing 2011;25: 1451-1468.

[25] Mao, L., Lu, Y. Extraction of artificial boundary frequencies for damage identification. Journal of Physics Conference Series 2011; 305: 1-10.

[26] Mao, L., Lu, Y. Selection of optimal artificial boundary condition (ABC) frequencies for structural damage identification. Journal of Sound and Vibration, 2016; 374: 245-259.

[27] He J., Fu Z. Modal analysis. Butterworth-Heinemann, Oxford, 2001.